Dual-Energy CT: Basic Principles, Technical Approaches, and Applications in Musculoskeletal Imaging (Part 1)

Patrick Omoumi, MD, MSc, PhD[1] Fabio Becce, MD[1*] Damien Racine, MSc[2] Julien G. Ott, MSc[2] Gustav Andreisek, MD, MBA[3] Francis R. Verdun, PhD[2*]

[1] Department of Diagnostic and Interventional Radiology, Lausanne University Hospital, Lausanne, Switzerland
[2] Institute of Radiation Physics, Lausanne University Hospital, Lausanne, Switzerland
[3] Institute for Diagnostic and Interventional Radiology, University Hospital Zurich, Zurich, Switzerland

Address for correspondence Patrick Omoumi, MD, MSc, PhD, Department of Diagnostic and Interventional Radiology, Lausanne University Hospital, Rue du Bugnon 46, CH-1011 Lausanne, Switzerland (e-mail: patrick.omoumi@chuv.ch).

Semin Musculoskelet Radiol 2015;19:431–437.

Abstract

In recent years, technological advances have allowed manufacturers to implement dual-energy computed tomography (DECT) on clinical scanners. With its unique ability to differentiate basis materials by their atomic number, DECT has opened new perspectives in imaging. DECT has been used successfully in musculoskeletal imaging with applications ranging from detection, characterization, and quantification of crystal and iron deposits; to simulation of noncalcium (improving the visualization of bone marrow lesions) or noniodine images. Furthermore, the data acquired with DECT can be postprocessed to generate monoenergetic images of varying kiloelectron volts, providing new methods for image contrast optimization as well as metal artifact reduction. The first part of this article reviews the basic principles and technical aspects of DECT including radiation dose considerations. The second part focuses on applications of DECT to musculoskeletal imaging including gout and other crystal-induced arthropathies, virtual noncalcium images for the study of bone marrow lesions, the study of collagenous structures, applications in computed tomography arthrography, as well as the detection of hemosiderin and metal particles.

Keywords

- dual-energy computed tomography
- crystal-induced arthropathies
- metal artifact reduction
- bone marrow edema
- iron

The concept of spectral imaging, or dual-energy computed tomography (DECT), is an old one, described by Godfrey Hounsfield in one of the first descriptions of CT in 1973.[1] This technique had already been suggested as a tool to differentiate tissue materials by using different X-ray spectra. The first applications of DECT to the musculoskeletal system date back to the late 1970s and early 1980s.[2–4] However, due to technological limitations, its implementation on clinical scanners was delayed until more recent years, particularly when dual-source CT was introduced in 2006.[5–8]

In the first part of this review article, we explain how DECT works including the different technical approaches currently available on the market, as well as radiation dose considerations.

Dual-Energy CT: How Does It Work?

DECT is based on the principle that the attenuation of tissues (reflected by their CT attenuation number in Hounsfield units [HUs]) depends on their density, but also on their atomic number Z, as well as on the energy of the photon beam. To understand how DECT works, we first review the basics of the interactions of the X-ray beam with tissues. The attenuation of tissues in CT is mainly due to two types of interactions

* F. Becce and F.R. Verdun contributed equally to this work.

Issue Theme Advances in Musculoskeletal Computed Tomography and Tumor Imaging; Guest Editor, Patrick Omoumi, MD, MSc, PhD

DOI http://dx.doi.org/10.1055/s-0035-1569253.
ISSN 1089-7860.

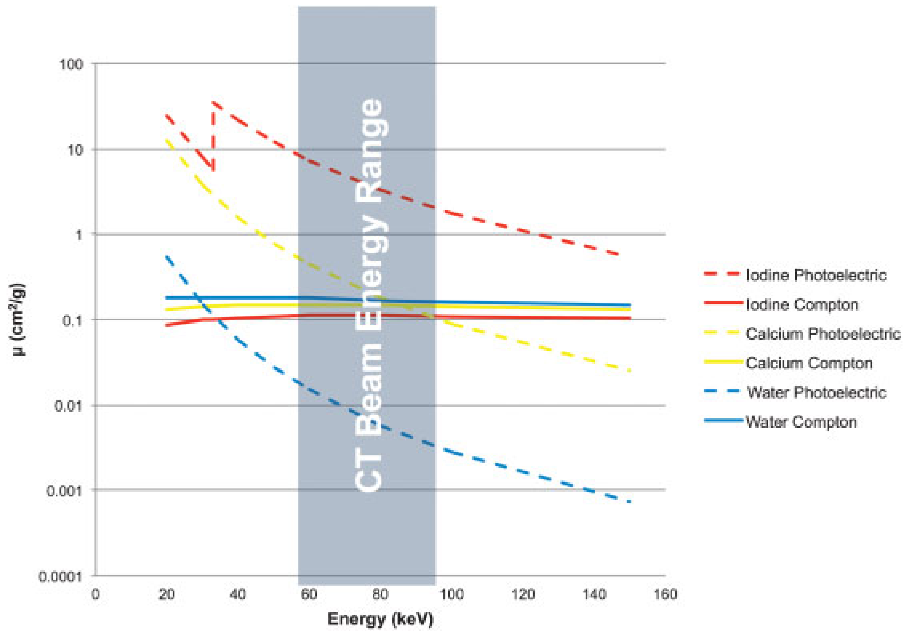

Fig. 1 Interactions of the X-ray beam with tissues. Photoelectric and Compton effects of various materials (iodine, calcium, and water) on attenuation level (μ [cm^2/g]), at different energy levels. In the range of photons' energies used in computed tomography (grayed area), the photoelectric effect, contrary to the Compton effect, strongly depends on the effective atomic number (Z_{eff}) of the material as well as on the energy of the photons.

between the X-ray beam and tissues: the photoelectric and the Compton effects. The Compton effect strongly depends on the electron density (ρ_e) of the material, which is correlated with mass density, but in the small range of photons' energies used in CT, the Compton effect does not depend on photon energy (►**Fig. 1**). The Compton effect is the main determinant of soft tissue contrast. The photoelectric effect, in contrast, strongly depends on the effective atomic number (Z_{eff}) of the material as well as on the energy of the photons. Lighter atoms, such as most atoms in soft tissues and water, do not present much of a photoelectric effect in the range of energies used in clinical CT scans. Calcium and iodine, however, are

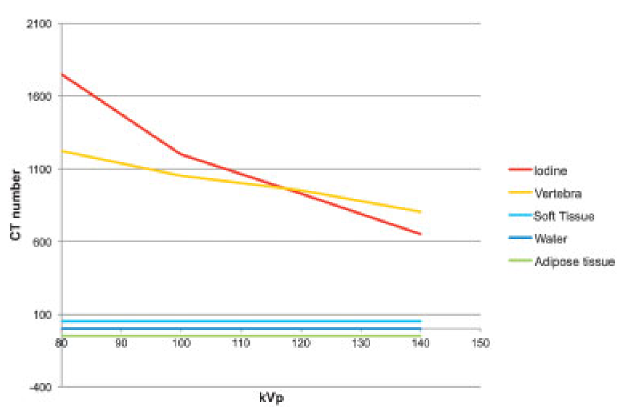

Fig. 2 Attenuation level (computed tomography number) of various components depending on the X-ray beam energy. The attenuation of higher Z materials such as calcium or iodine depends on beam energy levels, due to the photoelectric effect. This property can be used to differentiate those materials by combining the information obtained with two different energy levels of photons spectra.

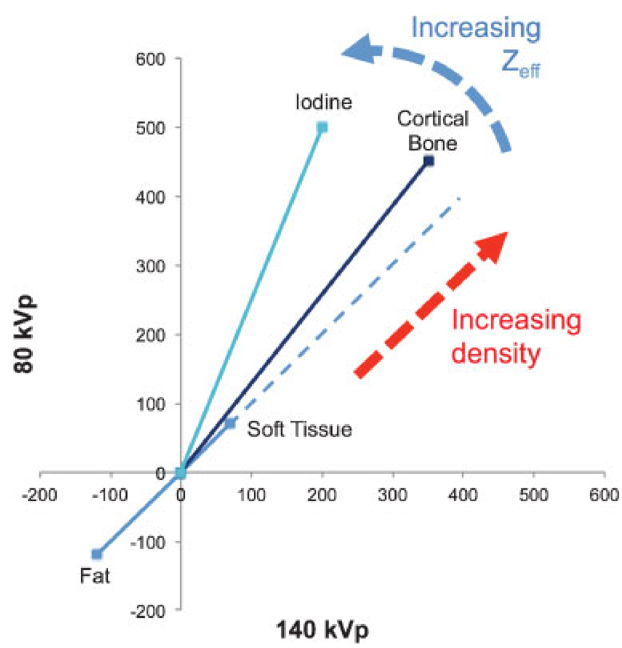

Fig. 3 Influence of the effective atomic number Z_{eff} on the attenuation (HU). The x-axis represents the HU value of a voxel at 140 kVp; the y-axis represents the HU value at 80 kVp. Each component is characterized by its slope, depending on Z_{eff}. The location of the value of a given voxel along this slope depends on the density of its components. The computed tomography (CT) number of water and soft tissues (which have comparable Z_{eff} values) is not energy dependent. Thus CT numbers of soft tissues will remain almost constant when varying the X-ray beam energy (thin dashed line). The location on this line will only depend on the density of the tissue (compare fat and soft tissue). For components with higher Z_{eff}, the photoelectric effect will come into play, and attenuation will be higher for lower energy levels (the higher the Z_{eff}, the steeper the slope).

susceptible to the photoelectric effect at lower energy levels, which can be exploited to differentiate those materials.

As seen in ►Fig. 2, the attenuation coefficient of higher Z materials such as calcium or iodine is higher for lower beam energy levels. This is due to the photoelectric effect. In ►Fig. 2, when using a single-energy level, such as the effective X-ray beam energy obtained at 120 kV, it is not possible to differentiate tissues containing calcium or iodine based on their attenuation level (both show CT numbers of $\sim$ 1,000 HU). However, when combining the information obtained by using two different energy levels of photon spectra (i.e., at effective energies produced when applying 80 and 140 kV), this differentiation can be made (iodine has a higher Z_{eff} than calcium, so its CT number is higher at a lower beam energy). To show graphically the influence of the Z_{eff} on CT numbers, it is convenient to represent the CT numbers at high and low energies as shown in ►Fig. 3. Because the photoelectric effect is highly dependent on Z_{eff}, the higher the Z_{eff}, the steeper the slope. The slope is a characteristic of the material, and the location of the value of a given pixel along this slope depends on density. Using these properties one can:

- Decompose attenuation coefficients into two basis-material components and generate basis-material density images[9] (►Fig. 4)
- Decompose the measured attenuation coefficients into Compton and photoelectric effects[10,11]
- Measure the Z_{eff} and ρ_e of each voxel[11,12] (►Fig. 5)
- Synthesize virtual monochromatic images at the desired energy level[13–15] (►Fig. 6)

To separate attenuation coefficients into two basis-material components and generate basis-material density images, we must remember that the CT number of water is not energy dependent. Thus CT numbers of soft tissues (with Z_{eff} values comparable to that of water) remain almost constant when varying the X-ray beam energy.

An example may illustrate the principle. A voxel contains a fraction f_A of material A and fraction f_B of material B. The goal is to assess f_A and f_B. To answer this, one must solve the simple set of two equations with two unknowns:

$$CT_{High} = f_A\, CT(A)_{High} + f_B\, CT(B)_{High}$$
$$CT_{Low} = f_A\, CT(A)_{Low} + f_B\, CT(B)_{Low}$$

CT_{High} and CT_{Low} are the CT numbers of the voxel measured, respectively, at high and low energies, so CT $(A)_{High}$ is the CT number of material A at high energy, and so on.

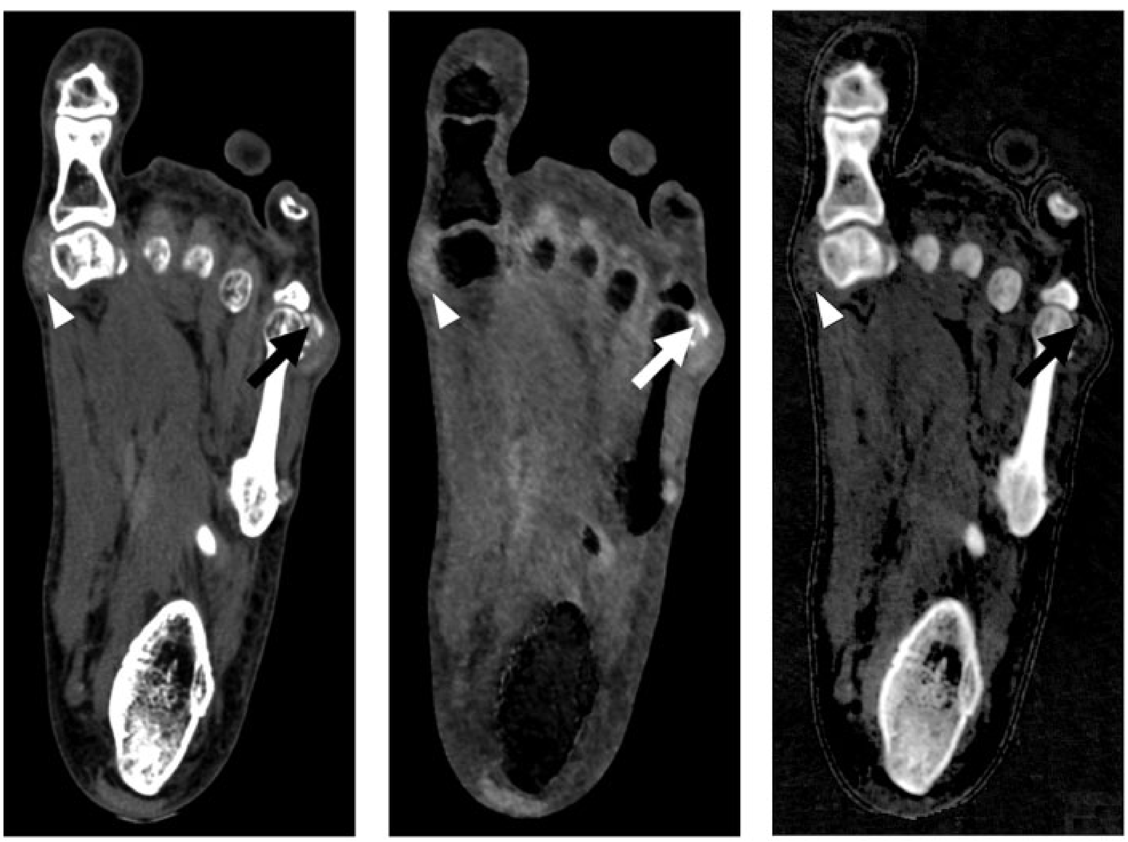

Fig. 4 A 35-year-old man referred by an orthopedic surgeon for acute pain and swelling in his left foot. (**a**) Conventional polychromatic computed tomography (CT) image shows indeterminate soft tissue masses around the first (arrowheads) and fifth (arrows) metatarsophalangeal joints, as well as the base of the fifth metatarsal bone, with CT numbers ranging from 150 to 200 HU and suggestive of gouty tophi. Basis-material (uric acid [**b**] versus calcium hydroxyapatite [**c**]) decomposition of dual-energy computed tomography data confirm the diagnosis of acute gout, with monosodium urate deposits of variable densities (arrows and arrowheads) visible on uric acid maps (b) and little calcium seen on the corresponding calcium hydroxyapatite images (c).

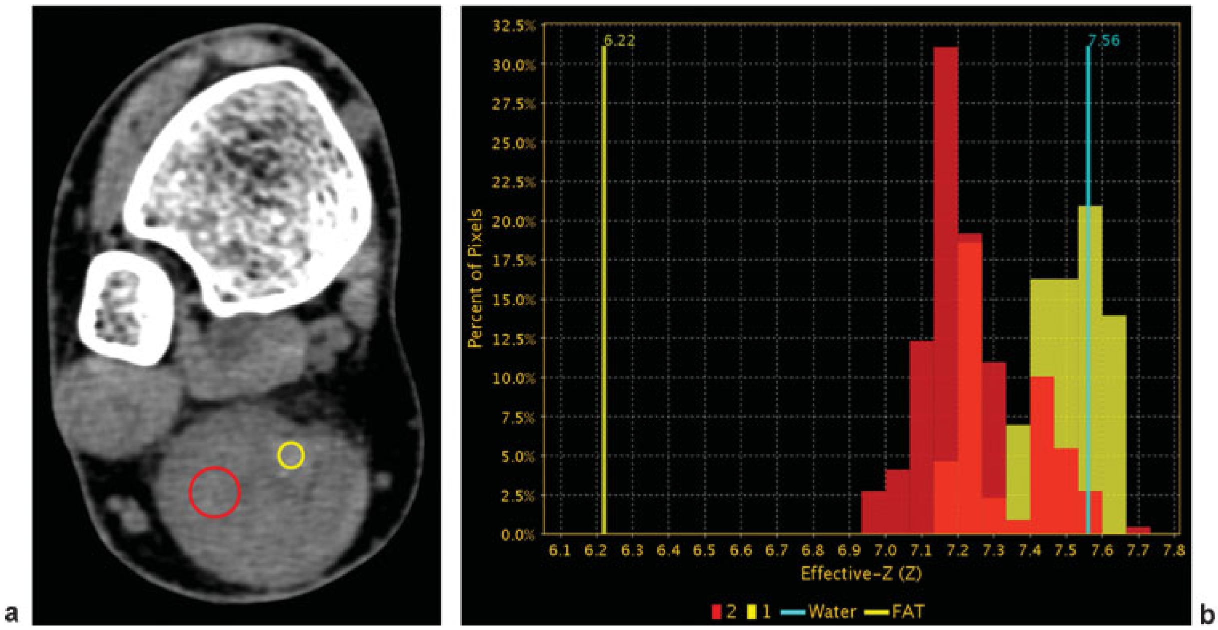

Fig. 5 A 40-year-old woman with no medical or family history, presenting with painless progressive swelling of both ankles. (**a**) Conventional computed tomography image of the right ankle shows diffuse nonspecific involvement of the Achilles and peroneal tendons. (**b**) Dual-energy computed tomography data offer the opportunity to measure the effective Z (Z_{eff}) of each voxel, allowing in this case to differentiate the normal tendon containing primarily water molecules (yellow histogram) from the abnormal tendon infiltrated by fatty tissue/xanthomas (red histogram).

To get the best material characterization, DECT should be performed in these conditions:

- Use two monochromatic (only one X-ray energy) beams with very different energy levels
- Acquire both data sets simultaneously
- Get images with the same quantity of photons on the detectors

However, CT technology is based on the use of conventional X-ray tubes that produce a spectrum of photons. The production of X-rays with this quite old technology remains

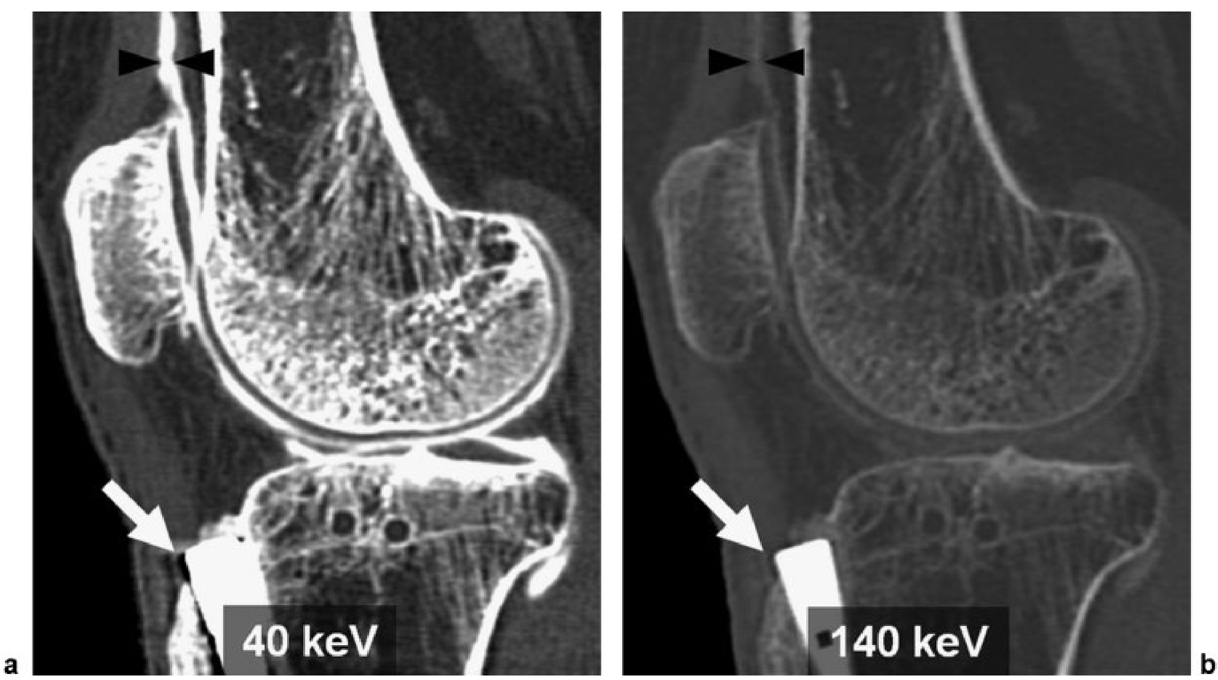

Fig. 6 A 27-year-old man with a history of tibial fracture treated with intramedullary nailing, presenting with chronic pain in the medial compartment of his right knee. Sagittal-reformatted virtual monoenergetic computed tomography arthrogram images at (**a**) 40 and (**b**) 140 keV (window level/width, 400/2000 HU, for both) reconstructed from dual-energy computed tomography (DECT) data. Note the gradual disappearance of intra-articular contrast material (25% iodine dilution, arrowheads), and the progressive reduction of streak metal artifacts (arrows), with increasing X-ray beam energy (adapted from Omoumi et al. article on DECT article Part 2 in this issue).[17]

the state of the art, but the use of a spectrum instead of monochromatic photons is associated with several limitations. The first one is beam hardening, which introduces a variation of the effective X-ray energy that depends on the quantity and type of material the beam will have to pass through. The second major limitation is the separation of the effective energies because X-ray spectra will always contain a fraction of low-energy photons. Another limitation of DECT resides in the need for heavy postprocessing, which is being standardized but remains time consuming.[16,18]

Three main types of algorithms are currently in use to postprocess DECT data sets[16]: (1) Image optimization algorithms usually provide three sets of images: two sets of monoenergetic images (typically at 80 or 100 keV and 140 keV), as well as an “optimum contrast” image from nonlinear blending of the low-energy images (providing high contrast) and high-energy images (providing low noise). (2) Differentiation algorithms allow the subtraction of a certain material from the data set, or the differentiation between two materials, through color coding, for example. (3) Quantification

Table 1 Basic principles, advantages, and disadvantages of currently available spectral imaging or dual-energy computed tomography techniques

	Spectral imaging technique (manufacturer)	Main advantages	Main limitations
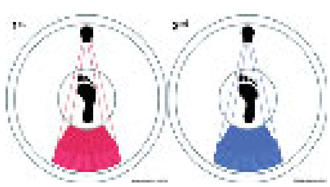	Sequential scans at low and high kilovolts (typically 80 and 140 kV) (All CT scanners with particular filtering strategies including Toshiba)	- Possible optimization of X-ray spectra to increase effective energy difference - Possible to get similar X-ray numbers at detector level	- Risk of patient motion between scans (projection data not paired)
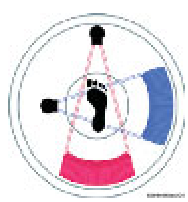	Dual-source CT (two X-ray tubes): low and high kilovolts acquired simultaneously (Siemens)	- Possible optimization of X-ray spectra to increase effective energy difference - Possible to get similar X-ray numbers at detector level - Radiation dose can be optimized through tube current modulation	- Projection data not paired (slight difference in acquisition time of the two data sets) - Space limitation inside the gantry (first-generation dual-source CT)
	Rapid kilovolt switching (typically 80 and 140 kV) (GE)	- Projection pairs possible by interpolation	- Impossible optimization of X-ray spectra to increase effective energy difference - Complex generator control - Tube current modulation not available - Difficult to get similar X-ray numbers at detector level
	One kilovolt with energy-discriminating detector (the top layer absorbs low-energy X-rays, whereas the bottom layer absorbs high-energy X-rays) (Philips)	- Perfectly paired projection data	- Imperfect energy discrimination - Difficult to get similar X-ray numbers at detector level
	One kilovolt with two filters in X-ray beam to achieve spectral separation (gold and tin filters) (Siemens)	- Projection pairs possible by interpolation	- Limited optimization of X-ray spectra to increase effective energy difference - Difficult to get similar X-ray numbers at detector level

Abbreviation: CT, computed tomography.

algorithms are based on three-material decompositions and for example can provide color-coded images of iodine content in postcontrast examinations.

The current spectral imaging or DECT techniques are based on the principles detailed in ►**Table 1**. Each approach has advantages and drawbacks that must be considered carefully. To date, no study has compared the diagnostic performance of these different techniques.

Radiation Dose Considerations in DECT

The radiation exposure required for DECT depends on the technology used. As discussed by Henzler et al, multiple studies have shown that dual-source DECT does not lead to increased radiation dose compared with conventional single-energy multidetector computed tomography. These data were mainly gathered from cardiac and chest applications.[19] This seems to also hold true for musculoskeletal applications. It has been shown that detection of bone marrow lesions in the knee and the ankle with dual-source DECT, using the virtual noncalcium technique, could be performed with a dose-neutral protocol (compared with conventional CT), taking advantage of the small cross-sectional scan area of the knee, compared with body applications.[20,21] For peripheral joints, a slight increase in radiation dose might not be a problem because the effective dose to these small anatomical structures, away from any radiosensitive organs, is negligible.[22]

With dual-source DECT, radiation dose reductions strategies include tube current modulation and the use of tin filters with the high-energy spectrum (to get rid of lower energy quanta and optimize the separation between the high- and low-energy spectra). The increased contrast of the lower energy spectrum can also be used to compensate for increased noise (keeping contrast-to-noise ratio levels constant).

For single-source DECT with rapid kilovolt switching, the radiation dose is usually higher than conventional monoenergetic CT, with ratios up to three times more radiation.[23] When matched for image quality assessed by low-contrast detectability, the radiation dose remains roughly 22% and 14% higher with single-source DECT with rapid kilovolt switching compared with conventional monoenergetic CT (evaluated for head and body examinations).[24] This is at least partly due to the nonavailability of tube current modulation with the rapid kilovolt switching technique.

For both dual-source and rapid kilovolt switching techniques, further radiation dose reduction is possible in various musculoskeletal conditions with the association of iterative reconstruction techniques with newer generation scanners[16,25–27] (see the dose optimization articles by Omoumi et al in this issue).[28,29] For other techniques of DECT, there is no or only scarce literature addressing radiation dose issues.

Conclusion

With its unique ability to differentiate basis materials by their atomic number, DECT has opened new perspectives in imaging. Used appropriately, it should not lead to an increase in radiation dose. Several image reconstruction algorithms have been developed to improve image contrast (i.e., by generating monoenergetic images), to characterize or subtract certain materials in the image, as well as to perform automatized volumetric measurements.

References

1 Hounsfield GN. Computerized transverse axial scanning (tomography). 1. Description of system. Br J Radiol 1973;46(552): 1016–1022
2 Fleischmann D, Boas FE. Computed tomography—old ideas and new technology. Eur Radiol 2011;21(3):510–517
3 Genant HK, Boyd D. Quantitative bone mineral analysis using dual energy computed tomography. Invest Radiol 1977;12(6):545–551
4 Kan WC, Wiley AL Jr, Wirtanen GW, et al. High Z elements in human sarcomata: assessment by multienergy CT and neutron activation analysis. AJR Am J Roentgenol 1980;135(1):123–129
5 Van Abbema JK, Van der Schaaf A, Kristanto W, Groen JM, Greuter MJW. Feasibility and accuracy of tissue characterization with dual source computed tomography. Phys Med 2012;28(1):25–32
6 Chinnaiyan KM, McCullough PA, Flohr TG, Wegner JH, Raff GL. Improved noninvasive coronary angiography in morbidly obese patients with dual-source computed tomography. J Cardiovasc Comput Tomogr 2009;3(1):35–42
7 Kalender WA, Buchenau S, Deak P, et al. Technical approaches to the optimisation of CT. Phys Med 2008;24(2):71–79
8 Flohr TG, McCollough CH, Bruder H, et al. First performance evaluation of a dual-source CT (DSCT) system. Eur Radiol 2006; 16(2):256–268
9 National Institute of Standards and Technology (NIST). NIST XCOM: Photon Cross Sections Database. Available at: http://www.nist.gov/pml/data/xcom/. Accessed December 3, 2015
10 Manohara SR, Hanagodimath SM, Thind KS, Gerward L. On the effective atomic number and electron density: a comprehensive set of formulas for all types of materials and energies above 1 keV. Nucl Instrum Methods Phys Res B 2008;266(18):3906–3912
11 Yang M, Virshup G, Clayton J, Zhu X, Mohan R, Dong L. WE-C-BRB-01: In vivo measurement of proton stopping power ratios in patients using dual energy computed tomography. Med Phys 2009;36:2757
12 Yang M, Virshup G, Clayton J, Zhu XR, Mohan R, Dong L. Theoretical variance analysis of single- and dual-energy computed tomography methods for calculating proton stopping power ratios of biological tissues. Phys Med Biol 2010;55(5):1343–1362
13 McCullough EC. Photon attenuation in computed tomography. Med Phys 1975;2(6):307–320
14 Hawkes DJ, Jackson DF. An accurate parametrisation of the x-ray attenuation coefficient. Phys Med Biol 1980;25(6):1167–1171
15 Henson PW. Determination of electron density, mass density and calcium fraction by mass of soft and osseous tissues by dual energy CT. Australas Phys Eng Sci Med 1989;12(1):3–10
16 Johnson TRC. Dual-energy CT: general principles. AJR Am J Roentgenol 2012;199(5, Suppl):S3–S8
17 Omoumi P, Verdun F, Guggenberger R, Andreisek G, Becce F. Dual-energy CT: basic principles, technical approaches, and applications in musculoskeletal imaging (Part 2). Semin Musculoskelet Radiol 2015;19(5):438–445
18 Schoepf UJ, Colletti PM. New dimensions in imaging: the awakening of dual-energy CT. AJR Am J Roentgenol 2012;199(5, Suppl): S1–S2
19 Henzler T, Fink C, Schoenberg SO, Schoepf UJ. Dual-energy CT: radiation dose aspects. AJR Am J Roentgenol 2012;199(5, Suppl): S16–S25

20 Pache G, Bulla S, Baumann T, et al. Dose reduction does not affect detection of bone marrow lesions with dual-energy CT virtual noncalcium technique. Acad Radiol 2012;19(12):1539–1545
21 Guggenberger R, Gnannt R, Hodler J, et al. Diagnostic performance of dual-energy CT for the detection of traumatic bone marrow lesions in the ankle: comparison with MR imaging. Radiology 2012;264(1):164–173
22 Biswas D, Bible JE, Bohan M, Simpson AK, Whang PG, Grauer JN. Radiation exposure from musculoskeletal computerized tomographic scans. J Bone Joint Surg Am 2009;91(8):1882–1889
23 Ho LM, Yoshizumi TT, Hurwitz LM, et al. Dual energy versus single energy MDCT: measurement of radiation dose using adult abdominal imaging protocols. Acad Radiol 2009;16(11):1400–1407
24 Li B, Yadava G, Hsieh J. Quantification of head and body CTDI(VOL) of dual-energy x-ray CT with fast-kVp switching. Med Phys 2011; 38(5):2595–2601
25 Tobalem F, Dugert E, Verdun FR, et al. MDCT arthrography of the hip: value of the adaptive statistical iterative reconstruction technique and potential for radiation dose reduction. AJR Am J Roentgenol 2014;203(6):W665–W673
26 Omoumi P, Verdun FR, Ben Salah Y, et al. Low-dose multidetector computed tomography of the cervical spine: optimization of iterative reconstruction strength levels. Acta Radiol 2014;55(3): 335–344
27 Becce F, Ben Salah Y, Verdun FR, et al. Computed tomography of the cervical spine: comparison of image quality between a standard-dose and a low-dose protocol using filtered back-projection and iterative reconstruction. Skeletal Radiol 2013;42(7):937–945
28 Omoumi P, Becce F, Ott J, Racine D, Verdun F. Optimization of radiation dose and image quality in musculoskeletal CT: emphasis on iterative reconstruction techniques (Part 1). Semin Musculoskelet Radiol 2015;19(5):415–421
29 Omoumi P. Verdun F. Becce F. Optimization of radiation dose and image quality in Musculoskeletal CT: emphasis on iterative reconstruction techniques (Part 2). Semin Musculoskelet Radiol 2015; 19(5):422–430